Microchim Acta (2016) 183:2473–2479
DOI 10.1007/s00604-016-1890-8

ORIGINAL PAPER

Enhanced Non-enzymatic amperometric sensing of glucose using $Co(OH)_2$ nanorods deposited on a three dimensional graphene network as an electrode material

Iman Shackery[1] · Umakant Patil[1] · Atiye Pezeshki[2] · Nanasaheb M. Shinde[1] · Seongil Im[2] · Seong Chan Jun[1]

Received: 21 February 2016 / Accepted: 31 May 2016 / Published online: 14 June 2016

Abstract We report on the synthesis of cobalt dihydroxide [$Co(OH)_2$] nanorods and their deposition on a 3-dimensional graphene network via chemical bath deposition. The structural characterization reveals deposited $Co(OH)_2$ to consist of flower-like nanorods on a 3-dimensional graphene foam. The nanocomposite was used for glucose sensing by electrocatalytic oxidation of glucose in 1 M KOH solution. Cyclic voltammetry and amperometric studies revealed a high sensitivity for glucose (3.69 mA mM^{-1} cm^{-2}) and a 16 nM detection limit. The nanocomposite offers a large effective surface (11.4 cm^2) and is very selective for glucose over potentially interfering materials such as dopamine, ascorbic acid, lactose, fructose and urea, not the least due to a relatively low working potential of 0.6 V (vs. Ag/AgCl). The high sensitivity, low detection limit and very good selectivity of free-standing nanocomposite electrodes are attributed to the synergistic effect of (a) the good electrocatalytic activity of the NRs, and (b) the large surface area with high conductivity offered by the 3D graphene foam.

Iman Shackery and Umakant Patil contributed equally to this work.

Electronic supplementary material The online version of this article (doi:10.1007/s00604-016-1890-8) contains supplementary material, which is available to authorized users.

✉ Seong Chan Jun
scj@yonsei.ac.kr

[1] School of Mechanical Engineering, Yonsei University, Seoul 120-749, Republic of Korea

[2] Institute of Physics and Applied Physics, Yonsei University, Seoul 120-749, Republic of Korea

Keywords Electro-oxidation · Amperometry · Cyclic voltammetry · Non-enzymatic glucose sensor · Chemical bath deposition

Introduction

Although the enzyme based glucose sensors show outstanding sensitivity and excellent selectivity, they suffer from some weaknesses such as the lack of stability due to the intrinsic nature of the enzymes. Several types of non-enzymatic glucose sensors have been developed [1, 2]. They are often based on the use of metal oxides and metal hydroxides, e.g. CuO [3], $Cu(OH)_2$ [4], MnO_2 [5], $Ni(OH)_2$ [6, 7], $Co(OH)_2$ [8] and CoO_x [9–12] which have been extensively investigated as the sensing materials for developing non-enzymatic glucose sensors. Among them, cobalt based electrodes has received much attention due to its electro-catalytic properties, well-defined electrochemical redox activity and chemical stability. Meanwhile, nanostructured $Co(OH)_2$ has a high specific surface and electroactive area, biocompatibility, excellent electronic conductivity, low cost and simple preparation process, that makes it suitable for high performance glucose detection. For instance, recently, He Mei et al. [13] reported Co@Pt core-shell nanoparticles display an electrocatalytic activity towards the oxidation of glucose at pH 7.0. Li Zhao et al. [14] achieves same pH for glucose sensing with Pt_3Pd nanoparticles. Above this achievements, KOH is still one of the good electrolytes for $Co(OH)_2$ due to stability of $Co(OH)_2$ in KOH.

Graphene foam known as three dimensional graphene (3DG), which consists of an interconnected network of graphene, is the direct synthesis of graphene macrostructures on nickel foam by chemical vapor deposition (CVD) [15]. The 3DG is commonly used in electrochemical sensors owing to their unique properties of chemical stability and large surface

area. Besides, three dimensional conducting porous structure provide high electrical conductivity with lightweight free standing framework. Generally the 3DG based sensors claim high sensitivity and low detection limit [10, 15] due to its three dimensional (3D) network that provides a greater surface area and more electroactive sites for spatial diffusion and interaction with target analytes. The 3D skeleton of a graphene network without any defects can efficiently overcome the strong π interaction and contact resistance between graphene sheets, consequently, offers higher conductivity and larger specific surface area compared to reduced graphene oxide sheets [15]. The unique properties of 3DG provides superior transfer of electrons which has a vital role in electrochemical sensors [16, 17].

Among various methods to prepare metal oxides and hydroxides, chemical bath deposition (CBD) is less elaborated, more controllable, cheaper and simpler. Although, the electrochemical behaviors and electrocatalytic activities of cobalt hydroxide/Graphene Foam ($Co(OH)_2$/3DG) has been studied for supercapacitor application [18, 19]. Till date, there has not been a systemic report on non-enzymatic glucose sensor based on it.

Herein, we report the synthesis of cobalt hydroxide [$Co(OH)_2$] nanorods (NRs) on three dimensional graphene (3DG) by chemical bath deposition (CBD) method, as non-enzymatic glucose sensor. The direct growth of $Co(OH)_2$ on 3DG need no more binder without any kinds of supporting substrate. The electrocatalytic activity of the nanocomposite, investigated by cyclic voltammetry (CV) and amperometric methods. The glucose sensing properties studied in terms of sensitivity, detection limit and selectivity toward Glucose. Also, the effective surface area and reproducibility of $Co(OH)_2$/3D graphene electrodes in presence of glucose is studied.

Experimental methods

Instrumentation, reagents and materials

Nickel foams (density ~480 g m^{-3}, thickness ~1.6 mm, Alantum Co. Ltd, South Korea, http://www.alantum.com/), etchant type CE-100 (Transene,USA, http://transene.com/etchants/), poly(methyl methacrylate) (PMMA) were used in the preparation of 3DG. To fabricate $Co(OH)_2$ nanorods, cobalt chloride hexahydrate ($CoCl_2$.6H2O), urea ($CO(NH_2)_2$) were purchased from Sigma-Aldrich (http://www.sigmaaldrich.com/). The materials for indicating the selectivity D-glucose, D-fructose, lactose, L-ascorbic acid (AA), and dopamine (DA) were obtained from Sigma-Aldrich (USA). All reagents were of analytical purity grade and directly used for experiments without any purification. All electrochemical measurements were carried out, using ZIVE SP2 LAB analytical equipment (South Korea) with three electrode configuration at room temperature (25 ± 3 °C). Deionized water (DI) was used in all experiments and growth of 3DG networks is done by chemical vapor deposition (CVD) as described in supporting information (see ESI).

Synthesis of $Co(OH)_2$ nanorods onto 3DG

After synthesizing 3DG by CVD (See ESI), 3DG were dipped in the mixture of 0.1 M cobalt chloride hexahydrate ($COCl_2.6H_2O$) as Co source and 0.1 M of Urea ($CO(NH_2)_2$) in DI water. The aqueous bath was heated at 95 °C for 6 h. Then the $Co(OH)_2$/3DG electrode was rinsed with DI and dried at room temperature. The pink colored $Co(OH)_2$/3DG (see optical image in Fig. 1) was used as working electrode in glucose sensing.

Apparatus and electrochemical measurements

The electrode materials were structurally characterized by XRD, XPS, TEM, FESEM, EDS, TGA (STA8000, PerkinElmer), FT-IR (Vertex70, Bruker) and Raman spectroscopy (LabRam Aramis, Horriba Jovin Yvon). The X-ray diffraction (XRD) was carried out on a Rigaku Smartlab diffractometer using Cu-Kα radiation. X-ray photoelectron spectroscopy (XPS) measurements were carried out on a thermo scientific ESCALAB 250 (Thermo Fisher Scientific, UK). The morphology of the composite was examined by transmission electron microscopy (TEM, JEM-2010, JEOL) and field-emission scanning electron microscopy (FESEM, JSM-7001 F, JEOL) coupled with EDS (Oxford, X-max).

The electrochemical sensing performances of $Co(OH)_2$/3DG electrodes were measured by conventional three-electrode system, which comprises with $Co(OH)_2$/3DG as working electrode, Ag/AgCl as reference electrode and platinum (Pt) as counter electrode in a 1 M KOH aqueous electrolyte. Cyclic Voltammetry (CV) and amperometric measurements were performed on the aforementioned workstation (ZIVE SP2 LAB analytical equipment, South Korea).

Result and discussion

The preparation and growing mechanism of $Co(OH)_2$/3DG is shown in Fig. 1 and a description is provided in SI (see the supporting information). During the preparation of 3DG, some ripples and wrinkles were shaped on the graphene films due to the difference between the thermal expansion coefficients of nickel foam and graphene. Also, during the chemical etching and other process some functional groups such as carboxyl groups were formed on the 3DG. As the temperature of solution bath increased to 95 °C, decomposition of urea (NH_2CONH_2) took place, producing

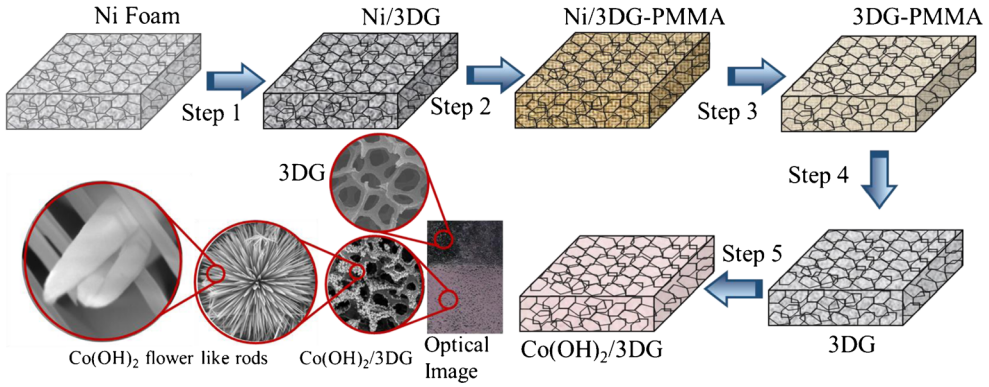

Fig. 1 Schematic of Synthesis of $Co(OH)_2$/3DG. *Step 1*: CVD growth of graphene films on Ni foam. *Step 2*: Coating a thin layer of PMMA on Ni/3DG *Step 3*: etching of nickel foam with FeCl3/HCl solution. *Step 4*: Dissolving the PMMA layer using acetone vapor. *Step 5*: Synthesis of $Co(OH)_2$ on 3DG. Optical image of $Co(OH)_2$/3DG and typical SEM image of 3DG and $Co(OH)_2$/3DG at different magnifications

CO_2 and NH_3 gradually. The ammonia reacts with cobalt ions of cobalt chloride hexahydrate ($CoCl_2.6H_2O$) precursor. Consequently, the amine complex metal ions ($Co(NH_3)_4^{2+}$) easily get adsorbed on the surface of the 3DG by electrostatic or Van-der Waals force. At the end the unstable $Co(NH_3)_4^{2+}$ formed metal hydroxide nanorods on the graphene surface. Subsequently, the growth of pink colored $Co(OH)_2$ take place on 3DG surface (see optical image in Fig. 1).

The demonstrated Raman spectrum of 3D graphene at different places on the foam exhibited two distinct peaks at ~ 1, 559 cm^{-1} and ~ 2,699 cm^{-1}, corresponding to G and 2D bands of graphene, respectively (See ESI, Fig. S1a) [20, 21]. The integral ratio of the 2D and G band indicates few layered domains containing 3DG. Especially, there is no peak of G band at around 1350 cm^{-1}, an indication of defects and disordered carbon, indicates that the CVD-grown 3DG has high quality and good conductivity [15].

Crystallinity of materials was studied using X-ray diffraction. The XRD patterns of 3DG and $Co(OH)_2$/3DG are shown in Fig. S1 (b) (See ESI). Two significant diffraction peaks (2θ) at 26.5° and 54.6° are attributed to the (002) and (004) reflections of the crystalline peak of hexagonal graphite carbon marked as 'O' (JCPDS: 75–1621). The XRD pattern of $Co(OH)_2$/3DG reveals that, characteristic peaks at ~ 17.02°(020), 23°(220), 33.5°(300), 34°(221), 34.4°(301), 39.1°(231), 46.8°(304) and 58.9°(412) and it can be indexed as cobalt hydroxide, which are consistent with the results in previous reports or standard card (JCPDS Card No. 38–0547) [22].

The thermogravimetric analysis (TGA) of 3DG and $Co(OH)_2$/3DG was carried out in air and the result is shown in Fig. S2 (a) (See ESI). The TGA curves shows the mass loss is about 97 % and 69 % in the range from room temperature to 450 ° C for 3DG and $Co(OH)_2$/3DG respectively. As can be seen from Fig. S2(a) (See ESI), almost both electrodes shows rapid mass loss between 300 and 405 °C. By using this method, it was estimated that the amount of $Co(OH)_2$ in the composite is around 28 % (weight ratio). To provide further evidence for the formation of $Co(OH)_2$/3DG during the CVD and CBD process, we characterized the $Co(OH)_2$/3DG and 3DG by Fourier transform infrared (FT-IR) spectroscopy (See ESI, S2b). The FT-IR data are similar to the data reported in the literatures, including strong peak of C = O at 1728 cm^{-1}, OH stretch at 3500.6 cm^{-1}. The broad bands at high frequency (3580–3400 cm^{-1}) and low frequency (800–400 cm^{-1}) indicate the presence of hydroxyl groups and water molecules in the $Co(OH)_2$/3DG electrodes [23, 24].

The XPS measurement was carried out to confirm the presence of $Co(OH)_2$. The Survey of XPS data is shown in Fig. 2a. The Fig. 2b represents the spectra of C(1 s) for $Co(OH)_2$/3DG electrode. The spectra of C(1 s) reveals that, peak centered at a binding energy of 284.88 eV represents C-C and C=C bonding and, along with shoulder peaks at 285.78, 286.28 and 288.78 eV can typically be assigned for the C-NR_2, C-O, COOH surface functional groups, respectively. To have detailed insight and the presence of hydroxide, O (1 s) core level of $Co(OH)_2$ was examined and the related fitted spectrum shown in Fig. 2c. It is observed that the O(1 s) core level region is composed of a broad peak cantered at 531.5 eV, which is associated with bound hydroxide groups (OH^-) and confirms the $Co(OH)_2$ formation rather than cobalt oxide on 3DG. As demonstrated in Fig. 2d, XPS spectra for Co (2p) of $Co(OH)_2$/3DG electrode indicates that, peaks of Co ($2p_{3/2}$) at 780.4 eV and Co ($2p_{1/2}$) at 796.48 eV are centered with a separation of 16.08 eV. These peaks are attributed to the presence of Co^{2+} chemical state as a clue for formation of $Co(OH)_2$ [25]. The existence of shake up satellite peaks of the Co ($2p_{3/2}$) and Co ($2p_{1/2}$) around 786.5 and 802.9 eV, respectively, confirmed the formation of Co^{3+} on the surface [26].

The morphologies of 3D graphene foam and $Co(OH)_2$/3DG examined by FESEM and shown in Fig. 3. The graphene foam is a 3D porous structure with a smooth and thin graphene

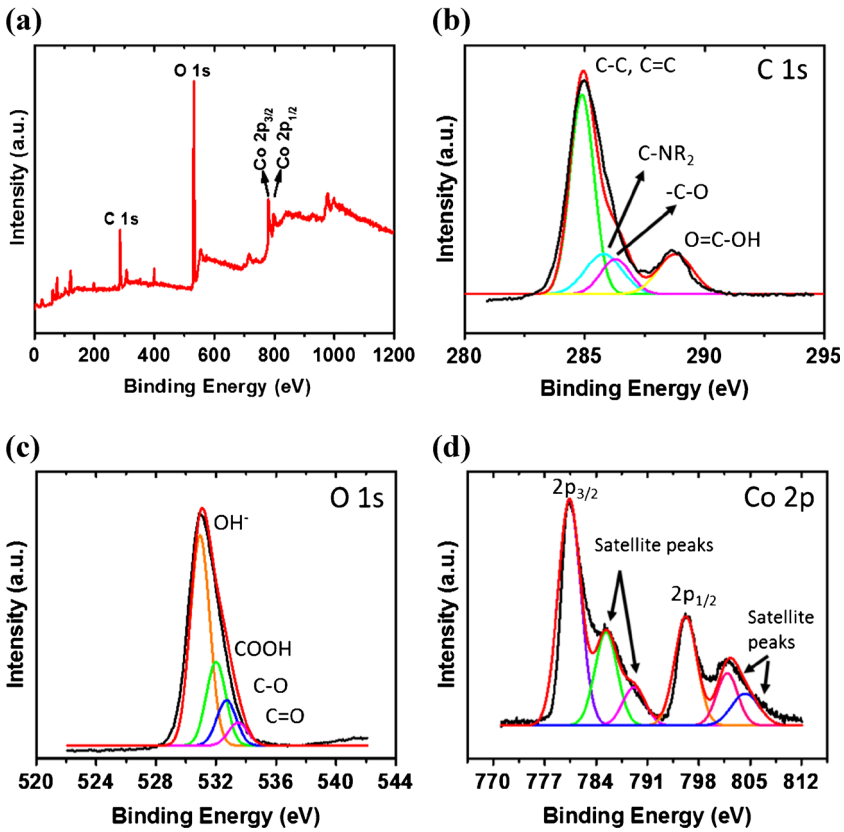

Fig. 2 XPS spectrum of **a** Co(OH)2/3DG and elemental spectra of **b** C 1 s, **c** O1s, **d** Co 2p

skeleton (Fig. 3a and b). The Fig. 3c and d) shows that, the twigs of graphene foam has been well covered by $Co(OH)_2$ NRs with overgrown particles at the edges. This overgrowth can be ascribed to a nucleation and coalescence process. The higher magnification image of the surface morphology in Fig. 3e, f reveals that the graphene sheet is well-covered with a vertically aligned flower-like structure. Also $Co(OH)_2$ nanorods are almost the same length with uniform distribution at the nanometer scale that offers abundant catalytic sites for glucose. Similar nanorods networks of $Co(OH)_2$/3DG were synthesized by Patil et al. [19]. The TEM image (Fig. 3f) inset) shows the width of $Co(OH)_2$ NR is about 45 nm. The FESEM and TEM analysis confirms that, the nanorods structure of $Co(OH)_2$ is formed on the graphene foam surface. Such

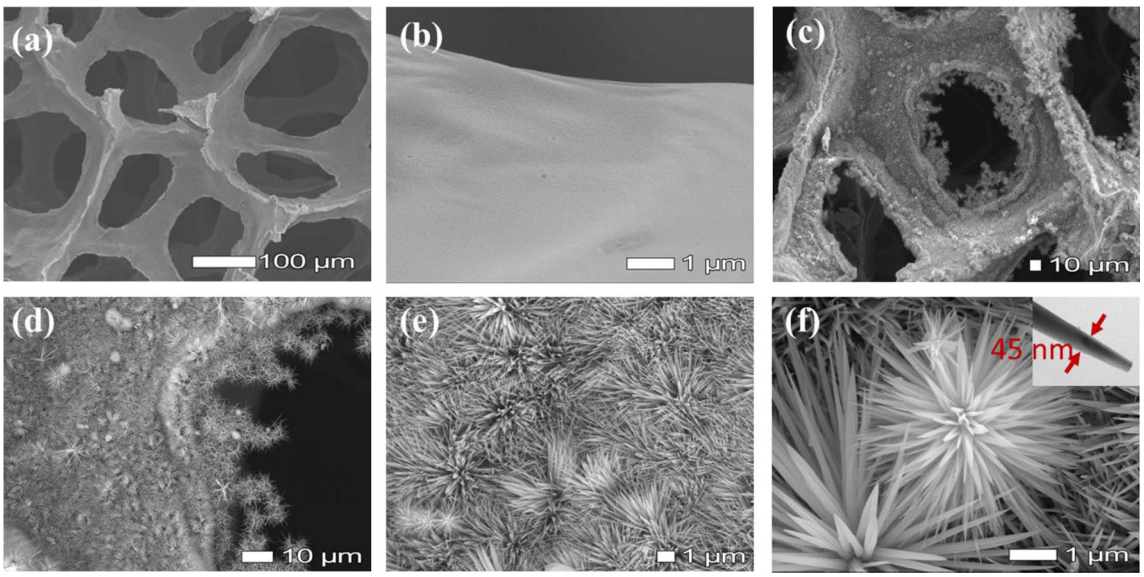

Fig. 3 **a**, **b** The SEM micrographs of graphene foam at different magnifications, **c**, **d**, **e** SEM micrographs of $Co(OH)_2$ on graphene foam at different magnifications. **f** SEM images of $Co(OH)_2$ nanorods on graphene surface at higher magnification. Inset of **f** shows TEM image of $Co(OH)_2$ nanorod

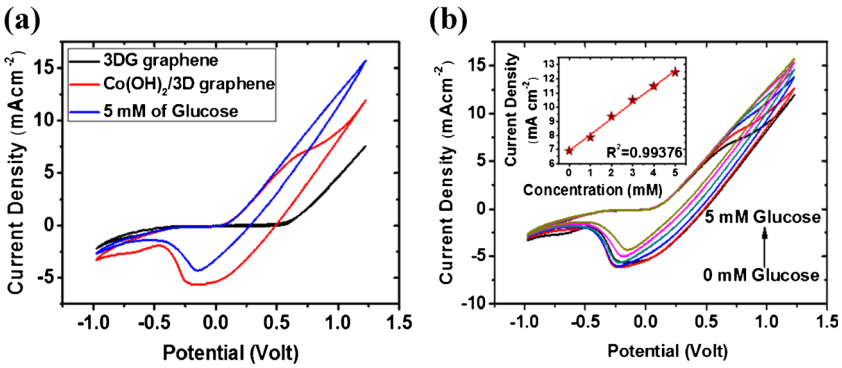

Fig. 4 **a** The electrocatalytic activities of 3DG and $Co(OH)_2$/3DG with and without 5 mM glucose at a scan rate of 20 mV s^{-1} in 1 M KOH. **b** The CV curve of $Co(OH)_2$/3DG at different concentration of glucose. The inset shows the linear range of the oxidation peak in the presence of various concentration of glucose

flower-like morphology leads to be a high specific surface area, which provides the structural foundation for the high sensitivity. The EDX element mappings and of carbon, oxygen, and cobalt atoms obtained from the SEM images of $Co(OH)_2$/3DG as shown in Fig. S1 (see ESI). The point EDX of 3DG shows 80 % of carbon with a little amount of Ni. This data indicates that almost all Ni was removed Fig. S2(a) (see ESI). The point EDX data of $Co(OH)_2$ flower like nanorods is demonstrated in Fig. S2(b) (see ESI).

A typical three-electrode system was employed with a saturated Ag/AgCl (3 M KCl) reference electrode, a Pt wire counter electrode, and the $Co(OH)_2$/3DG as working electrode. All potentials were referenced to Ag/AgCl (3 M KCl) electrode. Fig. S5 (a) (See ESI) shows the CV curves at different scan rates ranging from 10 to 100 mVs^{-1} for $Co(OH)_2$/3DG and in a aqueous 1 M KOH solution. All of the CV curves exhibit clearly two redox peaks arising from the reversible faradaic reaction in the alkaline electrolyte. The oxidation peak shows a significantly positive shift, and the reduction peak shifts negatively with the increase in scan rate which indicate that the redox reaction of $Co(OH)_2$ on graphene is rapid and reversible. Moreover, the Fig. S5 (b) (See ESI) shows anodic and cathodic peak vs. square root of scan rates that shows excellent linearity ($R^2 = 0.99017$ and 0.99707 for anodic and cathodic peak respectively). This result indicates that the redox reaction of $Co(OH)_2$ at the graphene surface is a typical diffusion-controlled electrochemical process [27]. The anodic peak in the positive scan detected at ~ 0.445 V (vs. Ag/AgCl) corresponds to an oxidation reaction $Co(OH)_2$ to CoOOH, while the cathodic peak in the negative scan which occurred around ~ −0.08 V (vs. Ag/AgCl) indicates the reverse process. The electrochemical reaction corresponding to the redox peaks can be expressed as follows [28]:

$$Co(OH)_2 + OH^- \overset{\text{Oxidationreduction}}{\longleftrightarrow} CoOOH + H_2O + e^- \quad (1)$$

The Fig. 4a shows the electrocatalytic activities of $Co(OH)_2$/3DG and 3DG which are investigated using cyclic voltammetry (CV) in a 1 M KOH solution with and without 5 mM glucose at a scan rate of 20 mV s^{-1}, that shows obvious electrocatalytic activity for glucose oxidation. No redox peaks can be observed in the cyclic voltammograms of 3DG skeleton, suggesting the $Co(OH)_2$/3DG electrode is suitable for high sensitivity electrochemical detection. Moreover, in the presence of 5 mM glucose, the anodic peak current from the $Co(OH)_2$/3DGF electrode is significantly higher than the composite electrode without glucose. Nevertheless, the behavior of the cathodic peak current is opposite. These experiment results suggest the outstanding catalytic properties of $Co(OH)_2$ toward the oxidation of glucose. The CV curve of $Co(OH)_2$/3DG at different concentration of glucose

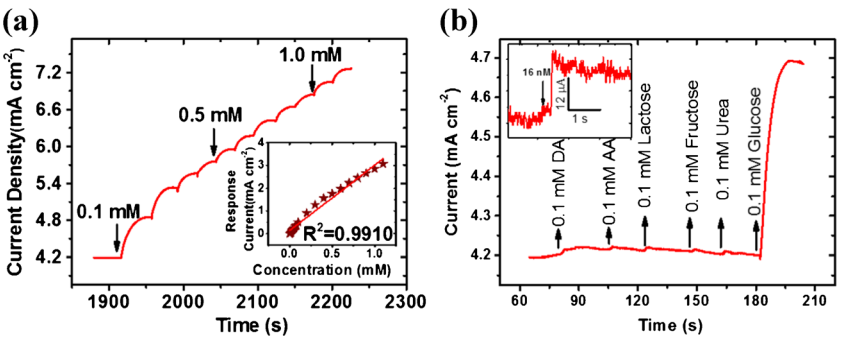

Fig. 5 **a** The typical amperometric (i-t) curve for $Co(OH)_2$/3DG electrode at an applied potential of 0.6 V in 1 M KOH. The inset shows graph of current response vs. glucose concentration **b** Selective determination of glucose at the $Co(OH)_2$/3DG electrode toward DA, AA, lactose, fructose, urea and glucose. The inset shows the response of $Co(OH)_2$/3DG electrode after adding 16 nM of glucose

from 0 to 5 mM is shown in Fig 4b. Upon the addition of glucose, a remarkable current and potential variation of the redox peaks are observed, while the oxidation peak has excellent linear range as demonstrated in inset of Fig. 4b. The oxidation of glucose to gluconolactone can be expressed by the $CoO(OH)/Co(OH)_2$ redox couple, according to the following reactions:

$$CoOOH + glucose \rightarrow Co(OH)_2 + gluconolactone \quad (2)$$

Additionally the shifting of redox peaks to the positive direction can be expressed as the absorption of glucose and the oxidized intermediates on the active side of electrode.

Effective surface area (ESA) measurements was performed with the same three-electrode configuration in an electrolyte solution of 3 M KCl containing 10 mM of $K_3Fe(CN)_6$ (potassium ferricyanide) at a variety of scan rates (see Fig. S6 (a)). Figure S6 (b) shows that the relationships between the peak current (I_p) and the square root of the potential scan rate ($v^{1/2}$) are almost linear ($R^2 = 0.98991$). ESA is estimated 11.4 $\pm$ 0.2 cm^2 from the Randles–Sevcik equation [29].

The typical amperometric i-t curve of $Co(OH)_2$/3DG at an applied potential of 0.6 v (potential around the anodic peak) is shown in Fig. 5a. A well-defined step-like increase for glucose response is observed with successive addition of 0.1 mM glucose. The $Co(OH)_2$/3DG shows a wide linear range, from 100 μM to 10 mM towards glucose determination with a correlation coefficient of 0.9910 (the inset of Fig. 5a). The sensitivity and detection limit is calculated to be 3.69 mA mM^{-1} cm^{-2} and 16 nM, respectively. The inset of Fig. 5b shows the response of $Co(OH)_2$/3DG electrode toward 16 nM of glucose.

A major challenge in glucose detection for a non-enzymatic glucose sensor is the electrochemical oxidation of meddling species such as DA, AA, lactose, fructose, and urea in physiological conditions. Figure 5b shows selective determination of glucose at the $Co(OH)_2$/3DG electrode by successive addition of 0.1 mM DA, AA, lactose, fructose, urea and glucose to 1 M KOH solution at an applied potential of 0.6 V. The addition of DA, AA, lactose, fructose, urea does not lead to any observable response or less than the response of glucose. The $Co(OH)_2$/3DG sensor shows very excellent performance in sensitivity, linear range and selectivity. The results demonstrate that the $Co(OH)_2$/3DG electrode is a promising candidate for non-enzymatic glucose determination.

Table 1 shows comparison of non-enzymatic glucose sensing performances based on various cobalt oxides/hydroxides based composites from previous reports and our present work. The sensitivity of our sensor is higher than previous reports and also detection limit is much less than the previous studies.

The reproducibility of the glucose sensor's measurement was also experienced with 5 different concentrations of glucose as shown in Table S1 (See SI). The calculated RSD values of the glucose were almost below 9 %, which indicates that the reproducibility of the sensors is practically acceptable [30, 31]. The reproducibility of $Co(OH)_2$/3DG electrodes also checked with same electrode in different concentration of glucose (See SI, Table S2). The $Co(OH)_2$/3DG electrodes with 3D porous structure, high sensitivity, low detection limit underlines its potential industrial application as a glucose sensors.

Conclusion

A non-enzymatic sensor made of $Co(OH)_2$ nanorods grown on 3DG by CBD method. The structural analysis reveals flower like structure of cobalt hydroxide nanorods (diameter ~45 nm) in nanocomposites of $Co(OH)_2$/3DG. The porous, conducting, chemical stable structure of 3DG play vital role in enhancement of glucose sensing application. Also, the unique $Co(OH)_2$ NRs morphology of electrode displays high sensitivity (3.69 mA mM^{-1} cm^{-2}), low detection limit (16 nM) and very good selectivity toward usual interfering materials such as dopamine (DA), Ascorbic acid (AA), lactose, fructose and urea in 1 M KOH electrolyte. The $Co(OH)_2$/3DG indicates a wide linear range, from 100 μM to 10 mM

Table 1 Comparison of non-enzymatic glucose sensing performances based on various cobalt oxides/hydroxides based composites which reported previously

Electrode	Sensitivity mA $mM^{-1}cm^{-2}$	Detection limit	Linear range	Selectivity	Ref.
Ni-Co hydroxide	0.122	–	0.25 μM ~ 3.7 mM	AA, UA, DA	8
3DG/Co_3O_4	3.39	25 nM	~80 μM	AA, UA	10
Co/Al hydrotalcite	0.424	–	0.002 ~ 1.5 mM	CA, UA, AP, AA	11
Co_3O_4 nanobiber	0.03625	97 μM	~2.4 mM	AA, UA	12
Co@Pt	0.00226	0.3 mM	1 ~ 30 mM	AA, UA, fructose, NaCl, AAP	13
3DG/$Co(OH)_2$	3.69	16 nM	100 μM ~ 10 mM	AA, UA, fructose, lactose, urea	This work

(DA) dopamine, *(AA)* Ascorbic acid, *UA* (Uric Acid), *CA* (Citric Acid), *AP* (Acetaminophen), *AAP* (Acetamidophenol)

towards glucose determination ($R^2 = 0.991$). The high sensitivity, low detection limit, very good selectivity and facile synthesis of $Co(OH)_2$/3DG composite electrodes can evoke its industrial application in glucose sensing devices.

Acknowledgements This work was partially supported by the Priority Research Centers Program (2009–0093823), the Korean Government (MSIP) (No. 2015R1A5A1037668) through the National Research Foundation of Korea (NRF) funded by the Ministry of Education, Science and Technology (MEST), and the Korea Research Fellowship Program funded by the Ministry of Science, ICT and Future Planning through the National Research Foundation of Korea (2015-11-1063).

Compliance with ethical standards The author(s) declare that they have no competing interests.

References

1. Chen X, Wu G, Cai Z, Oyama M, Chen X (2014) Advances in enzyme-free electrochemical sensors for hydrogen peroxide, glucose, and uric acid. Microchim Acta 181(7–8):689–705
2. Wang G, He X, Wang L, Gu A, Huang Y, Fang B, Geng B, Zhang X (2013) Non-enzymatic electrochemical sensing of glucose. Microchim Acta 180(3–4):161–186
3. Jiang L-C, Zhang W-D (2010) A highly sensitive nonenzymatic glucose sensor based on CuO nanoparticles-modified carbon nanotube electrode. Biosens Bioelectron 25(6):1402–1407
4. Shackery I, Patil U, Pezeshki A, Shinde NM, Im S, Jun SC (2016) Copper hydroxide nanorods decorated porous graphene foam electrodes for non-enzymatic glucose sensing. Electrochim Acta 191: 954
5. Chen J, Zhang W-D, Ye J-S (2008) Nonenzymatic electrochemical glucose sensor based on MnO_2/MWNTs nanocomposite. Electrochem Commun 10(9):1268–1271
6. Qiao N, Zheng J (2012) Nonenzymatic glucose sensor based on glassy carbon electrode modified with a nanocomposite composed of nickel hydroxide and graphene. Microchim Acta 177(1–2):103–109
7. Shackery I, Patil U, Song MJ, Sohn JS, Kulkarni S, Some S, Lee SC, Nam MS, Lee W, Jun SC (2015) Sensitivity enhancement in nickel hydroxide/3D-graphene as enzymeless glucose detection. Electroanalysis 27:2363–2370
8. Lien C-H, Chen J-C, Hu C-C, Wong DS-H (2014) Cathodic deposition of binary nickel-cobalt hydroxide for non-enzymatic glucose sensing. J Taiwan Inst Chem Eng 45(3):846–851
9. Heli H, Yadegari H (2010) Nanoflakes of the cobaltous oxide, CoO: synthesis and characterization. Electrochim Acta 55(6):2139–2148
10. Dong X-C, Xu H, Wang X-W, Huang Y-X, Chan-Park MB, Zhang H, Wang L-H, Huang W, Chen P (2012) 3D graphene–cobalt oxide electrode for high-performance supercapacitor and enzymeless glucose detection. ACS Nano 6(4):3206–3213
11. Scavetta E, Ballarin B, Tonelli D (2010) A cheap amperometric and optical sensor for glucose determination. Electroanalysis 22(4): 427–432
12. Ding Y, Wang Y, Su L, Bellagamba M, Zhang H, Lei Y (2010) Electrospun Co3O4 nanofibers for sensitive and selective glucose detection. Biosens Bioelectron 26(2):542–548
13. Mei H, Wu W, Yu B, Li Y, Wu H, Wang S, Xia Q (2015) Non-enzymatic sensing of glucose at neutral pH values using a glassy carbon electrode modified with carbon supported Co@ Pt core-shell nanoparticles. Microchim Acta 182(11–12):1869–1875
14. Zhao L, Wu G, Cai Z, Zhao T, Yao Q, Chen X (2015) Ultrasensitive non-enzymatic glucose sensing at near-neutral pH values via anodic stripping voltammetry using a glassy carbon electrode modified with Pt3Pd nanoparticles and reduced graphene oxide. Microchim Acta 182(11–12):2055–2060
15. Chen Z, Ren W, Gao L, Liu B, Pei S, Cheng H-M (2011) Three-dimensional flexible and conductive interconnected graphene networks grown by chemical vapour deposition. Nat Mater 10(6):424–428
16. Steiner M-S, Duerkop A, Wolfbeis OS (2011) Optical methods for sensing glucose. Chem Soc Rev 40(9):4805–4839
17. Wang J (2008) Electrochemical glucose biosensors. Chem Rev 108(2):814–825
18. Patil UM, Nam MS, Sohn JS, Kulkarni SB, Shin R, Kang S, Lee S, Kim JH, Jun SC (2014) Controlled electrochemical growth of Co(OH)2 flakes on 3D multilayered graphene foam for high performance supercapacitors. J Mater Chem A 2(44):19075–19083
19. Patil U, Lee SC, Sohn J, Kulkarni S, Gurav K, Kim J, Kim JH, Lee S, Jun SC (2014) Enhanced symmetric supercapacitive performance of Co (OH)2 nanorods decorated conducting porous graphene foam electrodes. Electrochim Acta 129:334–342
20. Ferrari A, Meyer J, Scardaci V, Casiraghi C, Lazzeri M, Mauri F, Piscanec S, Jiang D, Novoselov K, Roth S (2006) Raman spectrum of graphene and graphene layers. Phys Rev Lett 97(18):187401
21. Ferrari AC (2007) Raman spectroscopy of graphene and graphite: disorder, electron–phonon coupling, doping and nonadiabatic effects. Solid State Commun 143(1):47–57
22. Wang L, Dong ZH, Wang ZG, Zhang FX, Jin J (2013) Layered α-Co (OH) 2 Nanocones as electrode materials for Pseudocapacitors: understanding the effect of interlayer space on electrochemical activity. Adv Funct Mater 23(21):2758–2764
23. Pouchert CJ (1985) The aldrich library of FT-IR spectra. Aldrich Chemical Company, Milwaukee
24. Jayashree R, Kamath PV (1999) Electrochemical synthesis of α-cobalt hydroxide. J Mater Chem 9(4):961–963
25. Fu Z-W, Wang Y, Zhang Y, Qin Q-Z (2004) Electrochemical reaction of nanocrystalline Co 3 O 4 thin film with lithium. Solid State Ionics 170(1):105–109
26. Petitto SC, Marsh EM, Carson GA, Langell MA (2008) Cobalt oxide surface chemistry: the interaction of CoO (100), Co 3 O 4 (110) and Co 3 O 4 (111) with oxygen and water. J Mol Catal A Chem 281(1):49–58
27. Tyagi M, Tomar M, Gupta V (2014) Glad assisted synthesis of NiO nanorods for realization of enzymatic reagentless urea biosensor. Biosens Bioelectron 52:196–201
28. Jagadale A, Jamadade V, Pusawale S, Lokhande C (2012) Effect of scan rate on the morphology of potentiodynamically deposited β-Co (OH) 2 and corresponding supercapacitive performance. Electrochim Acta 78:92–97
29. Bard AJ, Faulkner LR (1980) Electrochemical methods: fundamentals and applications, vol 2. Wiley, New York
30. Li G, Liao J, Hu G, Ma N, Wu P (2005) Study of carbon nanotube modified biosensor for monitoring total cholesterol in blood. Biosens Bioelectron 20(10):2140–2144
31. Song MJ, Kim JH, Lee SK, Lim DS, Hwang SW, Whang D (2011) Analytical characteristics of electrochemical biosensor using Pt-dispersed graphene on boron doped diamond electrode. Electroanalysis 23(10):2408–2414